J MATER SCI **41** (2006) 1547–1556

High-pressure phase equilibria in binary and ternary mixtures with one near- or supercritical and one high-molecular component. New insights for application and theory

T. KRASKA*
Department of Physical Chemistry, University of Cologne, Luxemburger Str. 116, D-50939 Cologne, Germany
E-mail: t.kraska@uni-koeln.de

D. TUMA
Department of Mechanical and Process Engineering, University of Kaiserslautern, P. O. Box 30 49, D-67653 Kaiserslautern, Germany
E-mail: tuma@rhrk.uni-kl.de

In this work we report on two different high-pressure phase equilibria. The first is the solubility of a low-volatile solid in a supercritical phase. These are two anthraquinone dyes 1,4-bis-(hexadecylamino)-9,10-anthraquinone and 1,4-bis-(dodecylamino)-9, 10-anthraquinone dissolved in CO_2 and N_2O. Secondly, the partition of an infinitely diluted high-molecular biocompound between coexisting high-pressure liquid phases in a ternary system consisting of a nearcritical gas, water, and an organic solvent, that is a fully miscible with water at standard conditions, is investigated. The high-molecular compounds are two cardiac glycosides digoxin and digitoxin, which occur in the foxglove plant. The corresponding ternary phase-forming system consists of CO_2, water, and 1-propanol. The binary solubilities are determined within 310 and 340 K and up to 180 MPa where retrograde solubility is observed. The partitioning experiments are done at 313 and 333 K and at pressures, where a three-phase liquid-liquid-gas equilibrium with one water-like and one propanol-like phase exists. Experimental data are listed and discussed. Additionally, the correlation of the solubility data with a recently developed Carnahan-Starling-van der Waals type equation of state extended for the nearcritical region are discussed. The partitioning data with a hybrid model that combines the Peng-Robinson equation of state with an excess Gibbs energy approach based on UNIQUAC are outlined briefly and the results interpreted.

1. Introduction

The need for environmentally sound processes was the promoter for supercritical fluids into many fields of application. The astonishing properties of supercritical fluids especially, their large variability, can achieve results that other technologies cannot. Actually, supercritical fluids expand into new fields of application [1], for example, downstream processes in biotechnology. The majority of processes can be summarized under the term "extraction". A recurring theme always is a reliable knowledge of phase behavior, since binary, ternary, and even higher systems are invariably encountered in practical applications. Multicomponent high-pressure phase behavior is known to be rather complicated, often multifaceted in their appearance; therefore, there is a strong need for experimental studies over a broad pressure and temperature range.

In many applications, particularly in the field of biotechnology, high-molecular compounds must be treated. This work shall contribute some insights into high-pressure phase equilibria in binary, ternary, and

*Author to whom all correspondence should be addressed.
0022-2461
DOI: 10.1007/s10853-006-4644-x

pseudoternary mixtures with a supercritical gas and a solute of high molar weight. The two case studies both deal with extraction. At first, we present solubility data of high-molecular organic dyestuffs (alkylated anthraquinone derivatives) in supercritical solvents up to distinguishing high pressures together with a recently developed correlation model [2, 3]. The substances fulfil the criterion of low volatility very well and typify surrogates for poorly soluble high-molecular biomolecules. Their handling during investigation, however, is much easier, and the anthraquinone dyestuffs have thus been chosen as model substances. The experiments reported have encountered the region of retrograde solubility at liquid-like densities of the compressed gas. Our correlation performs well describing this phenomenon.

The second part comprises the partitioning of a biomolecule on coexisting water-like liquid phases. Pure supercritical fluids are often known to be rather poor solvents, as the previously reported results have shown. A possibility to circumvent extreme pressures or temperatures is to utilize the liquid-liquid phase split of water and a completely water-soluble organic solvent, preferably lower alkanols like, e.g., ethanol and propanol, upon pressurization with a so-called "nearcritical" gas like CO_2 or ethene [4]. Such ternary systems exhibit this phase split at relatively mild conditions. "Nearcritical" means in this context near, typically a little above the critical temperature of the solvent gas, which meets the demands of sensitive components.

Digitalis drugs are used to treat congestive heart failure and heart rhythm irregularities. The different digitalis glycosides are closely comparable concerning pharmacodynamics but differ substantially in regard to pharmacokinetics. Digoxin, being less lipophilic, shows lower protein binding and shorter half-life, is mainly eliminated via kidney, and thus accumulates rather rapidly in people with insufficient kidney function. Digitoxin, however, is more lipophilic and extensively bound to plasmaproteins, has a longer half-life, is mainly eliminated in metabolized state via urine and does not accumulate in kidney dysfunction [5, 6]. Therefore, separation is a must from the medical standpoint because of the incidence of toxic side effects. Here, the feasibility for extraction and separation of a pair of structurally similar pharmaceutical agents is outlined. Additionally, an attempt to correlate the partitioning behavior is discussed.

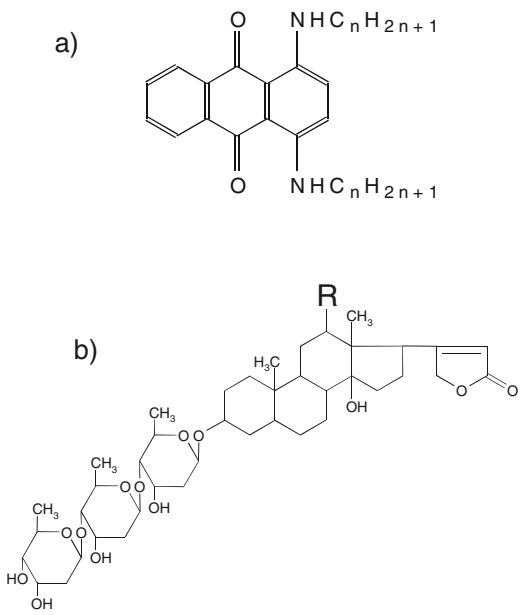

Figure 1 Structures of the low-volatile solutes investigated here: (a) dispersion dyes 1,4-bis-(*normal*-alkylamino)-9,10-anthraquinone, $n = 12$ for AQ12 (dodecyl) and $n = 16$ for AQ16 (hexadecyl); (b) foxglove cardenolides digitoxin and digoxin, R = H for digitoxin and R = OH for digoxin.

2. Experimental section

The procedures for determining the solubility of 1,4-bis-(hexadecylamino)-9,10-anthraquinone (AQ16) and 1,4-bis-(dodecylamino)-9,10-anthraquinone (AQ12) in the two supercritical gases CO_2 and N_2O are described in the paper by Swidersky *et al.* [7]. These experiments were performed within *p*,T-boundaries as follows: 310.0 K $\leq T \leq$ 340.0 K and 10.0 MPa $\leq p \leq$ 30.0 MPa for AQ12 + CO_2, 310.0 K $\leq T \leq$ 330.0 K and 7.6 MPa $\leq p \leq$ 12.7 MPa for AQ12 + N_2O, 320.0 K $\leq T \leq$ 340.0 K and 15.0 MPa $\leq p \leq$ 180.0 MPa for AQ16 + CO_2, 310.0 K $\leq T \leq$ 330.0 K and 10.0 MPa $\leq p \leq$ 160.0 MPa for AQ16 + N_2O [7, 8]. The method was analytical in-situ VIS-spectroscopy. Swidersky *et al.* also found a melting temperature $T_{fus} = 352$ K for AQ12 and 366.5 K for AQ16, respectively. Melting points were determined visually in a melting tubule according to the method of Tottoli [8].

The partitioning experiment of the two cardiac glycosides digitoxin (Dt) and digoxin (Dg) on coexisting liquid phases in the ternary system CO_2 + water + 1-propanol was part of a doctoral thesis [9], and data are reported in the paper by Adrian *et al.* [10]. Here, the experiments were done at the two temperatures 313.15 and 333.15 K and within the pressure boundaries of 7.055 MPa $\leq p \leq$ 14.1 MPa for $T = 313.15$ K and 10.10 MPa $\leq p \leq$ 16.12 MPa for $T = 333.15$ K.

The structures of the high-molecular compounds are illustrated in Fig. 1.

3. Results and discussion

3.1. *The binary systems or high-pressure equilibrium solubility of a low-volatile compound in a supercritical fluid*

Fig. 2 illustrates our experimental data for the solubility of AQ12 in CO_2 together with the calculated solubility isotherms. The corresponding solubility data are listed in Table I. The solubility isotherms show a monotonously

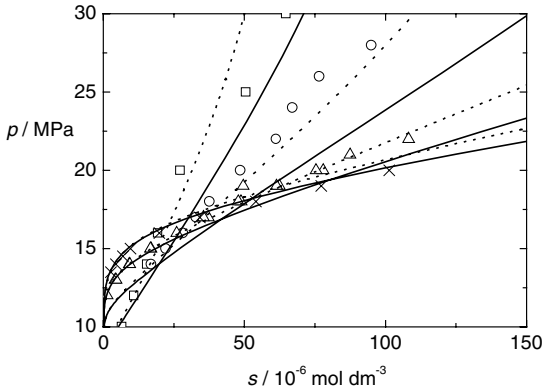

Figure 2 Solubility of AQ12 in supercritical CO_2. The symbols are the experimental data at the following temperatures: $T = 310.0$ K (□), $T = 320.0$ K (○), $T \leq 330.0$ K (△), $T \leq 340.0$ K (×). The curves belong to the correlation: solid = interpolated parameter, dashed = parameter from global fit.

increasing solubility towards higher pressures. Higher temperatures make the increase distinctly steeper. If solubility is plotted versus density, the intersections between the isotherms disappear but the monotonous solubility increase with higher densities is kept. A test for supersaturation at $T = 340$ K (pressure jump from 20 to 13.5 MPa) was negative.

Compared to AQ16 the solubility of the higher homologue AQ16 in N_2O, shown in Fig. 3 and listed in Table II, is much lower, so that we could tap the full pressure range (up to 200 MPa) of the equipment.

Retrograde solubility behavior is observed at high solvent densities for all temperatures investigated like in the corresponding system with AQ18 (the octadecylamino derivative) acting as solute [11]. Supersaturation was checked for all temperatures, for example, at $T = 330$ K the solubility at $p = 25$ MPa was directly recorded after the value at $p = 170$ MPa. Fig. 3 shows that the data point fits into the isotherm very well. In previous studies, systematic CO_2-solubility investigations on bisubstituted anthraquinone derivatives of this type with either a stepwise elongation of the alkyl chain (from methyl (AQ01) to octyl (AQ08)) or with branched substituents (1-methylethyl (AQiso03)) were performed. The corresponding results are published in Fluid Phase Equilibria, together with the behavior of more polar anthraquinone derivatives. Any continuative information concerning experiment and data can be drawn from the references cited therein [12]. Referring to this classification, the solubility in CO_2 (at a fixed temperature) monotonously decreases in the order AQ08, AQ12, AQ16, and finally AQ18 [7, 12].

Figs. 4 and 5 show the results for the solubility of AQ12 and AQ16 in supercritical N_2O. The corresponding data go with Tables I and II. To exchange CO_2 by the isosteric N_2O gives the known effect of increasing the solubility significantly. This effect, which occurred both for AQ12 and AQ16, was observed for other anthraquinone derivatives, too [7, 11, 12, 14]. N_2O always increased the solubility of the solutes under isothermal treatment without any exception so far, but the shape of the isotherms remains similarly here including that a plot solubility versus solvent density shows no intersections of the isotherms. Due to the higher solubility, the analysable pressures were bound to rather low pressures. The solubility isotherm of AQ16 in N_2O at 310 K (cf. Fig. 5, the solubility was low enough to continue towards higher pressures), however, looks quite unusual. The familiar steep solubility increase flattens quite

TABLE I Experimental solubility data of AQ12 in CO_2 and N_2O. Density values refer to the pure solvent; they were calculated according to reference [13] for CO_2 and reference [2] for N_2O, respectively.

p/MPa	ρ/kg m^{-3}	s/10^{-6} mol dm^{-3}	p/MPa	ρ/kg m^{-3}	s/10^{-6} mol dm^{-3}
$T = 310.0$ K; CO_2			$T = 320.0$ K; CO_2		
10.0	685.8	6.54	14.0	703.3	16.86
12.0	749.8	10.85	15.0	726.3	22.11
14.0	787.8	15.39	16.0	746.3	28.19
16.0	815.5	19.28	17.0	763.0	32.84
20.0	856.3	27.22	18.0	777.6	37.57
25.0	893.3	50.49	20.0	802.3	48.49
30.0	922.0	64.71	22.0	822.9	61.16
			24.0	840.7	67.03
$T = 330.0$ K; CO_2			26.0	856.3	76.45
12.0	476.6	1.27	28.0	870.3	95.00
13.0	546.5	4.23			
13.0	546.5	4.53	$T = 340.0$ K; CO_2		
14.0	597.5	9.24	13.5	458.8	2.68
14.0	597.5	9.43	14.0	486.6	4.47
14.0	597.5	9.44	14.5	512.2	6.87
15.0	635.5	16.94	15.0	535.6	9.63
15.0	635.5	16.74	16.0	575.7	19.86
16.0	665.2	26.04	17.0	608.6	34.21
17.0	689.5	37.23	18.0	636.1	54.09
17.0	689.5	35.52	19.0	659.4	77.19
18.0	710.0	48.82	20.0	679.7	101.28
18.0	710.0	47.83			
19.0	727.7	62.43	$T = 320.0$ K; N_2O		
19.0	727.7	61.42	9.0	445.7	5.37
19.0	727.7	59.62	9.5	515.6	13.37
20.0	743.3	77.95	10.0	565.7	23.87
20.0	743.3	75.45	10.5	602.0	38.78
21.0	757.2	87.38	11.0	629.6	62.71
22.0	769.8	108.24	11.0	629.6	59.36
			11.5	651.7	76.56
$T = 310.0$ K; N_2O					
7.6	601.6	10.55	$T = 330.0$ K; N_2O		
7.6	601.6	11.15	10.0	386.7	2.33
8.0	644.4	19.51	10.5	429.8	5.36
8.5	675.9	27.93	11.0	469.6	11.32
9.0	698.2	38.38	11.5	505.1	26.47
9.5	715.7	46.03	11.8	524.2	37.25
9.5	715.7	45.11	12.0	536.0	44.58
10.0	730.3	60.76	12.3	552.6	58.01
10.5	742.8	66.78	12.5	562.9	69.49
11.0	753.8	77.77	12.7	572.6	77.08
11.5	763.7	82.21			

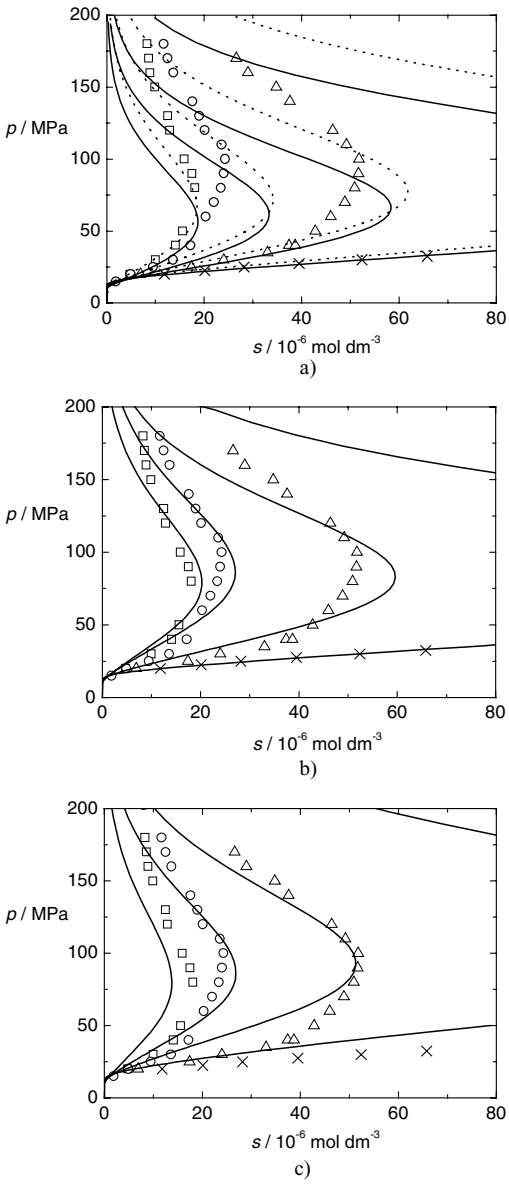

Figure 3 Solubility of AQ16 in supercritical CO_2. The symbols are the experimental data at the following temperatures: $T = 320.0$ K (□), $T = 325.0$ K (○), $T = 330.0$ K (△), $T = 340.0$ K (×). The curves belong to the correlation. (a) solid = interpolated parameter, dashed = parameter from global fit; (b) solid = parameter fitted to each temperature separately; c) solid = parameter from a single fit at $T = 325.0$ K.

abruptly at approximately 50 MPa to continue in this way towards higher pressures. Besides, in contrast to CO_2, the test for supersaturation revealed the following results: The system AQ12 + N_2O showed no supersaturation at $T =$ 310 K. The other temperatures were not tested, but measurements were strictly performed in the recommended manner by a stepwise pressure increase. AQ16 + N_2O exhibited strong supersaturation at 310 and 320 K, but the effect surprisingly did not occur at 330 K. To ensure reliability of the 310 K-isotherm, measurements were repeated several times with fresh gas portions.

TABLE II Experimental solubility data of AQ12 in CO_2 and N_2O. Density values refer to the pure solvent; they were calculated according to reference [13] for CO_2 and reference [2] for N_2O, respectively.

p/MPa	ρ/kg m^{-3}	s/10^{-6} mol dm^{-3}	p/MPa	ρ/kg m^{-3}	s/10^{-6} mol dm^{-3}
$T = 320.0$ K; CO_2			$T = 325.0$ K; CO_2		
20.0	802.3	4.83	15.0	683.1	1.87
30.0	883.0	9.99	20.0	773.5	4.91
40.0	933.7	14.06	25.0	825.5	9.47
50.0	971.6	15.61	30.0	863.0	13.63
80.0	1050.3	18.11	40.0	917.2	17.16
90.0	1070.2	17.47	60.0	989.0	20.26
100.0	1088.1	15.94	70.0	1015.8	21.98
120.0	1119.5	12.93	80.0	1039.0	23.40
130.0	1133.4	12.48	90.0	1059.5	24.01
150.0	1158.6	9.94	100.0	1077.9	24.33
160.0	1170.1	8.90	110.0	1094.7	23.57
170.0	1181.0	8.61	120.0	1110.1	20.08
180.0	1191.4	8.35	130.0	1124.3	19.04
			140.0	1137.6	17.58
$T = 330.0$ K; CO_2			160.0	1161.8	13.73
20.0	743.3	6.92	170.0	1172.9	12.51
25.0	801.8	17.37	180.0	1183.5	11.67
30.0	842.7	24.01			
35.0	874.4	32.98	$T = 340.0$ K; CO_2		
40.0	900.6	37.38	20.0	679.7	11.84
40.0	900.6	38.72	22.5	720.7	20.13
50.0	942.6	42.84	25.0	752.7	28.21
60.0	975.9	45.96	27.5	779.0	39.51
70.0	1003.7	48.89	30.0	801.2	52.42
80.0	1027.7	50.90	32.5	820.6	65.77
90.0	1048.8	51.66			
100.0	1067.8	51.85	$T = 320.0$ K; CO_2		
110.0	1084.9	49.16	13.0	700.0	12.00
120.0	1100.7	46.36	15.0	742.0	17.27
140.0	1128.9	37.62	17.5	779.6	27.33
150.0	1141.6	34.76	20.0	808.0	40.79
160.0	1153.6	29.04	22.5	830.7	49.63
170.0	1164.9	26.60	25.0	850.0	63.41
			26.5	860.3	67.03
$T = 310.0$ K; CO_2			28.0	869.8	75.27
10.0	730.2	5.76			
10.0	730.2	4.71	$T = 330.0$ K; CO_2		
10.0	730.2	5.61	13.0	586.0	9.20
12.0	772.6	8.53	14.0	625.0	15.77
12.0	772.6	7.80	16.0	679.9	36.03
15.0	814.2	16.75	17.0	701.0	47.66
15.0	814.2	15.12	17.5	710.4	56.64
16.0	825.1	19.57	18.0	719.1	66.96
20.0	860.4	28.77	19.0	735.0	78.80
22.5	878.0	33.49			
25.0	893.4	35.14			
40.0	959.8	48.57			
50.0	991.1	53.29			
50.0	991.1	52.54			
60.0	1016.8	55.63			
60.0	1016.8	55.94			
70.0	1038.8	56.31			
70.0	1038.8	58.44			
80.0	1058.2	60.47			
90.0	1075.4	61.21			
90.0	1075.4	63.11			
90.0	1075.4	63.25			
100.0	1091.0	64.45			
100.0	1091.0	64.54			
110.0	1105.3	65.76			
130.0	1130.9	68.01			
150.0	1153.2	71.57			
160.0	1163.5	71.97			

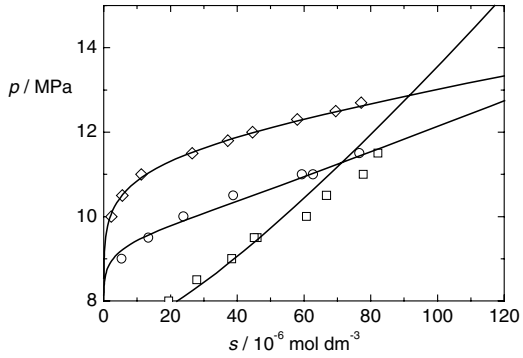

Figure 4 Solubility of AQ12 in supercritical N_2O. The symbols are the experimental data at the following temperatures: $T = 310.0$ K (□), $T = 320.0$ K (○), $T = 330.0$ K (◇). The curves are the correlations done by a global parameter fit.

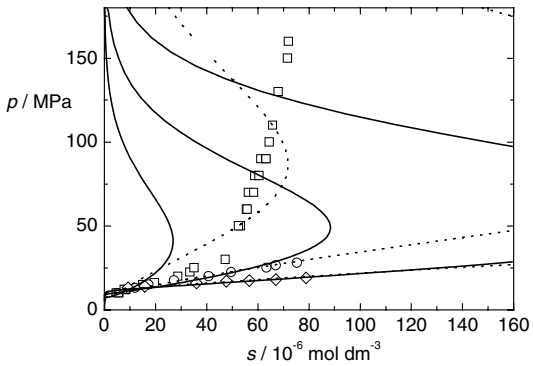

Figure 5 Solubility of AQ16 in supercritical N_2O. The symbols are the experimental data at the following temperatures: $T = 310.0$ K (□), $T = 320.0$ K (○), $T = 330.0$ K (◇). The curves are the correlations done by a global parameter fit; solid = fit without high-pressure data (high-pressure data for $p \leq 50$ MPa), dashed = fit with high-pressure data.

In all Figures the results of the correlation are included. Correlation data are available from the authors. In the following paragraph the main characteristics of our equation of state model shall be outlined. The underlying equation of state is a—non-cubic—Carnahan-Starling-van der Waals type equation of state that is corrected by an additional term improving the near-critical behavior. The major reason to refrain from using a cubic equation of state to correlate the solubility of a low-volatile solute in a supercritical solvent is their poor performance to model the *pVT*-behavior of the solvent in the critical region. The parameters become afflicted with flaws therefrom, and during the handling with a second component, as in the solubility correlation, it is likely that extrapolating to distinctively high pressures or the backward estimation of solute properties becomes inaccurate. The equation of state employed here circumvents such problems by an additional perturbation term improving the description of the *pVT*-behavior in the critical region.

The backbone of the equation of state is a reference term built from a Carnahan-Starling repulsion term and a modified van der Waals attraction term together with the perturbation term. For conceptual, procedural, and mathematical details of the model the reader is referred to recent papers [2, 3, 11]. By the employment of a fugacity approach [15], the equation becomes suitable for binary mixtures with low-volatile (and low-soluble) solutes, for details again see [2, 3, 11]. This approach requires solute properties which can be treated as adjustable parameters if data are not available from somewhere. These are the molar volume of the pure solute $V_{m,s}$, the saturation pressure p_{sat}, and the isothermal compressibility κ_T. The temperature dependence of the saturation pressure p_{sat} is described via a Clapeyron-type function including two parameters A_{sat} and B_{sat}. The data source for fitting these parameters are the solubility data sets at different temperatures. At least, mixing rules for the equation-of-state parameters are required for a mixture. In our model, we use quadratic one-fluid mixing rules, which contribute the adjustable cross parameters k_{12} and l_{12} (where the index 1 represents the solvent and 2 the solute, respectively). T^*_{22} is the attraction parameter and b_{22} the volume parameter of the pure solute. Table III lists the complete set of parameters which were employed during this study.

Two papers deal with solubility correlations of this particular anthraquinone family so far [11, 16]. The results of those correlations were quite satisfactory, for example, describing and predicting the coordinates of a solubility maximum. Here, shown in Figs. 2 and 3a, solubility isotherms for the two systems AQ12 + CO_2 and AQ16 + CO_2 were at first correlated with interpolated parameters. The solubility behavior in CO_2 for AQ12 and AQ16 is in between AQ08 and AQ18, so we expected reasonable results. The quality of the correlation is already acceptable. We obtained the parameters via fitting an exponential function (for $V_{m,s,}$ b_{22}, A_{sat}, and B_{sat}) or a quadratic polynomial (for T^*_{22}) to the results from the solubility data of the systems AQ03 + CO_2 [16], AQ08 + CO_2 [16], and AQ18 + CO_2 [11]. The best coincidence (mean average relative deviation) between experiment and correlation was found for both systems at $T = 340$ K (10.8% for AQ12 + CO_2 and 6.7% for AQ16 + CO_2). The region of maximum solubility in the system AQ16 + CO_2, however, was afflicted by a significantly higher discrepancy. Next, we determined the parameters in the usual way by fitting to all isotherms simultaneously (the so-called "global fit"). The correlation improved thereupon for AQ12 (Fig. 2), and also slightly for the system AQ16 + CO_2 (Fig. 3a). The discrepancy between experiment and correlation for AQ12 + CO_2 now ranged from 4.6% at $T = 330$ K to 14.6% at $T = 310$ and 340 K. It improved less for the system AQ16 + CO_2, especially for the region of retrograde solubility. In case of AQ16 + CO_2 (cf. Figs. 3b and 3c) we tested two other possibilities, namely a correlation for each temperature separately (cf. Fig. 3b, the deviation between 4.2% at $T =$ 340 K and 22.0 % at $T = 320$ K) and a correlation solely

TABLE III Adjusted parameters of the equation of state and solute parameters. The corresponding correlations are illustrated in the figures indicated. For all correlations κ_T is zero.

System	T^*_{22}/K	b_{22}/cm^3 mol^{-1}	k_{12}	l_{12}	A_{sat}/K	B_{sat}	$V_{m,s}$/cm^3 mol^{-1}
AQ12 in CO_2, interpolated (Fig. 2)	734.663	147.70	1.0	1.0	18066.62	25.335	520.25
AQ12 in CO_2, global fit (Fig. 2)	713.954	145.49	1.0	1.0	17852	25.335	520.25
AQ16 in CO_2, interpolated (Fig. 3a)	685.601	159.15	1.0	1.0	19448.3	27.459	552.25
AQ16 in CO_2, global fit (Fig. 3a)	688.791	153.884	1.0	1.0	19407.6	27.459	552.52
AQ16 in CO_2: correlation for each temperature separately (Fig. 3b)							
at 320.0 K	704.798	150.535	1.0	1.0	19592.4	27.459	556.363
at 325.0 K	672.169	151.205	1.0	1.0	19374.8	27.459	567.139
at 330.0 K	687.944	152.624	1.0	1.0	19439.1	27.459	556.575
at 340.0 K	686.419	157.670	1.0	1.0	19453.4	27.459	561.010
AQ12 in N_2O, global fit (Fig. 5)	733.971	141.877	1.0	1.0	17756.9	25.5345	520.25
AQ16 in N_2O, global fit with high-pressure data (Fig. 6)	713.437	136.014	1.0	1.0	18977.7	28.2739	552.25
AQ16 in N_2O, global fit without high-pressure data (Fig. 6)	702.325	154.814	1.0	1.0	19418.5	27.9656	552.25

on the parameters fitted to the isotherm at $T = 325$ K (cf. Fig. 3c). The latter accounted better for the high-pressure region, yet the results fall short of those for AQ18 + CO_2 [11].

The corresponding N_2O-correlations (cf. Figs. 4 and 5) manifest as follows: For the system AQ12 + N_2O the global fit performs very well (between 5.2% at $T = 340$ K and 14.0% at $T = 320$ K). However, it shall be kept in mind here that the experiments restrict to a maximum pressure of ≈ 13 MPa only.

The same picture can be seen for the low pressures in the system AQ16 + N_2O. The course of the high-pressure correlation for the single isotherm for $T = 310$ K showed that under consideration of the high-pressure data ≥ 50 MPa for 310 K there exists a maximum which does not deviate very much from the experiment in the solubility value, but the course indicates the maximum at pressures beyond our experiments. Generally, the correlation predicts for both solvents a similar shape for the high-pressure region, which is not in agreement with the data of the 310 K-isotherm. So, an extension of the data basis is desired.

Ultimately, we want to take a view on the correlation parameters (in CO_2 only) when plotted against the side-chain length AQn of these molecules. These plots are illustrated in Fig. 6. All data except those for the melting temperature T_{fus} were obtained from the so-called "global fit", which means one temperature independent parameter set for one system. $V_{m,s}$ and B_{sat} for AQ12 and AQ16 were interpolated via the exponential function, i.e., the numbers exactly match the curve. The two volume parameters $V_{m,s}$ and b_{22} shown in the subdiagram increase monotonously as expected. The value for AQ02 from crystal structure analysis [17] fits in here. A similar trend is found for the parameters related to the saturation pressure A_{sat} and B_{sat}, as shown in Figs. 6b and d. The attraction parameter of the pure solute T^*_{22}, however, increases in the region of short alkyl chains, passes a maximum and drops with a higher n. The melting temperature T_{fus} of the pure solute, which is also shown there, gives almost the opposite trend. A possible explanation of the particular T^*_{22}-behavior might be that the long alkyl chains are known to be flexible [12], and so the polar oxygen atom can be shielded by the weakly interacting side chains. The melting point will be determined by interaction of various effects, for example, investigations proved polymorphism in the solid state [12].

3.2. *The ternary and pseudoternary systems or infinite dilution partition coefficient of a high-molecular biomolecule on coexisting liquid phases in a ternary system*

A ternary mixture of CO_2, water, and 1-propanol belongs to the particular systems "nearcritical" gas + water + organic solvent, which reveal a liquid-liquid phase split at elevated pressures, commonly called "salting out". Here, the employed gas is the salting out agent. When such a three-phase equilibrium is observed at a certain temperature, its existence is limited to a certain pressure region between a so-called lower (LCEP) and upper critical endpoint (UCEP) of two characteristical critical lines. When going up on the pressure axis we observe that first at the LCEP ($L_1 = L_2$) this three-phase equilibrium originates, then the composition of the water-rich (L_1) and vapor phase (V) do not change their composition very much, whereas the composition of the solvent-rich phase (L_2) is shifted towards the vapor phase by uptaking the gas. Ultimately, the three-phase equilibrium ceases to exist at the UCEP ($L_2 = V$). At higher pressures we enter a single two-phase

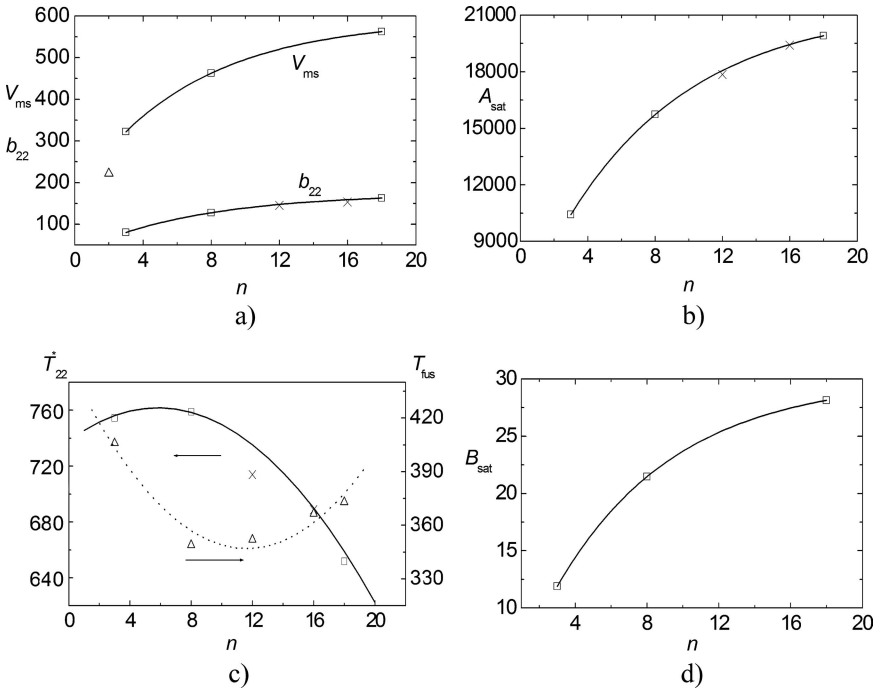

Figure 6 Correlated equation of state parameters and properties of the pure solid in CO_2 as function of the chain length n of the anthraquinone dyes AQn: (a) molar volume of the pure solute $V_{m,s}$ and the equation of state parameter b_{22}. The triangle is the molar volume of AQ02 as obtained by X-ray diffractometry [17]; (b) parameter A_{sat} of the temperature dependence of the saturation pressure; (c) equation of state parameter T^*_{22} and the melting point T_{fus} [12]; (d) parameter B_{sat} of the temperature dependence of the saturation pressure.

liquid-liquid equilibrium of the persisting water-rich and a gas-rich—fluid—phase with a density to be suitable for extraction. The present work deals with the partitioning of biomolecules on both liquid phases of such a phase equilibrium. Besides, much more complicated phase equilibria are likely to occur in those ternary systems [4], such as two simultaneously existing three-phase equilibria or a four-phase equilibrium. A comprehensive study on phase equilibria in the system CO_2 + water + 1-propanol was reported by Adrian *et al*. [18] followed by two investigations of the partitioning of various different biomolecules on coexisting liquid phases therein [19, 20].

Figs. 7 and 8 show both experimental and modelled results for the partitioning of the two foxglove ingredients digoxin and digitoxin in a plot $K^{(x)}$ vs. Π with the corresponding data given in Table IV. The partition coefficient of a solute is defined as the ratio of the molar fractions in the two coexisting liquid phases: $K_i^{(x)} = c_i^{(L_2)}/c_i^{(L_1)}$. This reduced pressure Π was introduced to compare different temperatures (since the coordinates of LCEP and UCEP are temperature-dependent) in a single diagram. The coordinates of the critical endpoints were as follows [10, 18]: at $T = 313.15$ K $p_{LCEP} = 6.784$ MPa and $p_{UCEP} = 15.00$ MPa; at $T = 333.15$ K $p_{LCEP} = 9.753$ MPa and $p_{UCEP} = 16.74$ MPa. With this definition at the starting point $p = p_{LCEP}$ (both liquid phases are critical) $K^{(x)} = 1$. $K^{(x)} > 1$ means a preference for the solvent-rich phase L_2 or lipophilicity, whereas the opposite $K^{(x)} < 1$ preference for L_1 and thus hydrophilicity. The investigated pair of biomolecules is structurally indeed very similar, but rather different in their preference towards solvent characteristics, as the diagrams show. The OH-substituted digoxin (cf. Fig. 1) is more hydrophilic than digitoxin having a hydrogen atom at this position. Anyway, from the amount of substance introduced into the ternary mixture the main part goes into the phase L_2 (since $K^{(x)} > 1$ at all conditions). In these experiments, the amount of fourth component did not exceed about 0.1 g per kilogram of feed solution, so that the phase behavior of the phase-forming system remained unaffected by the fourth component. Data for the composition of the L_1L_2 V-equilibrium are reported in the study done by Adrian *et al*. [10]. The resulting mixture can be regarded as a pseudo-ternary mixture. The effect of temperature on the partition coefficients is subordinate to the effect of pressure.

Both substances are scarcely soluble in water. The maximum solubility in pure solvents at normal pressure and $T = 313.1$ K yielded for digoxin: 0.0195 g dm^{-3} in water (density ρ of the saturated solution = 992 g dm^{-3}), 6.05 g dm^{-3} in methanol (775 g dm^{-3}), 1.03 g dm^{-3} in 1-propanol (789 g dm^{-3}), and 1.32 g dm^{-3} in 1-butanol (796 g dm^{-3}). For digitoxin it was found: 0.00579 g dm^{-3} in water (density ρ of the saturated solution = 992 g dm^{-3}), 19.8 g dm^{-3} in methanol (781 g dm^{-3}), 12.4 g dm^{-3} in 1-propanol (792 g dm^{-3}), and 6.95 g dm^{-3} in 1-butanol (797 g dm^{-3}).

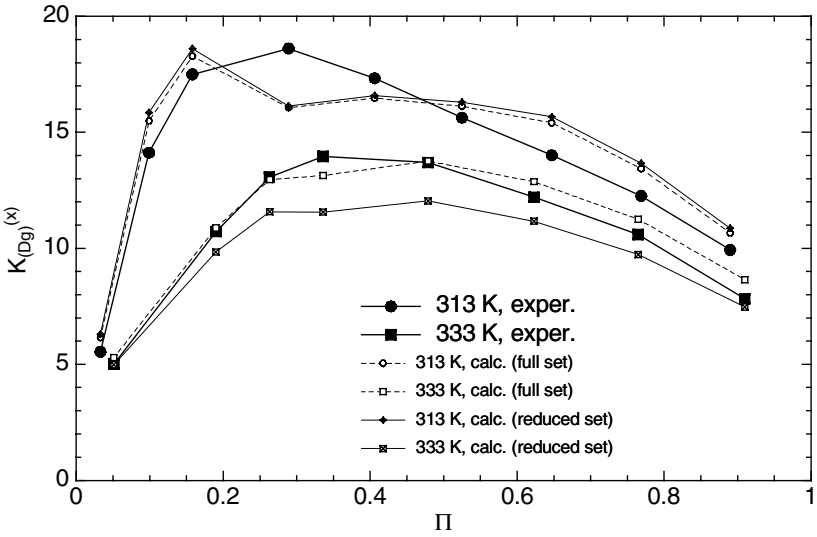

Figure 7 Infinite dilution partition coefficient $K^{(x)}$ of digoxin (Dg) in coexisting liquid phases of the three-phase equilibrium L_1L_2V in the ternary system CO_2 + water + 1-propanol as a function of reduced pressure, $\Pi = (p - p_{LCEP}) / (p_{UCEP} - p_{LCEP})$. The filled symbols represent experimental data, the open symbols results from the model.

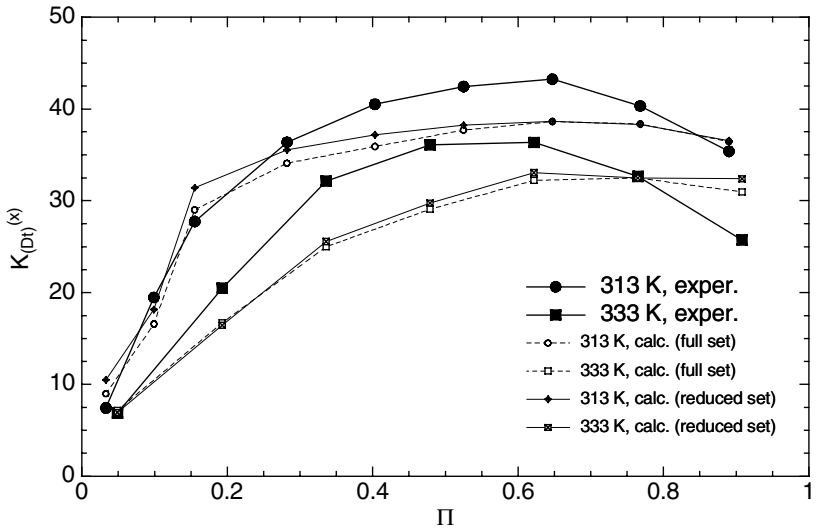

Figure 8 Infinite dilution partition coefficient $K^{(x)}$ of digitoxin (Dt) in coexisting liquid phases of the three-phase equilibrium L_1L_2V in the ternary system CO_2 + water + 1-propanol as a function of reduced pressure, $\Pi = (p - p_{LCEP}) / (p_{UCEP} - p_{LCEP})$. The filled symbols represent experimental data, the open symbols results from the model.

Since the separation factor α, i.e., the ratio of both partition coefficients $\alpha_{Dg,Dt} = K_{Dt}^{(x)}/K_{Dg}^{(x)}$ differs from unity and increases with higher pressures, a separation process utilizing this ternary system in principle is possible. In the aforementioned paper [10], Adrian *et al*. outlined exemplary extraction processes in a countercurrent column for separating both glycosides. Such a different liquid-liquid extraction might be an alternative where a supercritical extraction perhaps is disadvantageous, because the process conditions remain mild and the dissolving power of an organic solvent can be utilized.

Adrian developed a model to correlate such partition coefficients [9] and applied it successfully to describe the distribution of a high-molecular biocompound to the present ternary system CO_2 + water + 1-propanol prior to this study [19]. Here, the same model was applied (cf. Figs. 7 and 8); it shall be outlined in brief, since the procedure details and the mathematical background can be drawn from the References [9, 19, 20]. The model combines an equation of state (here, the—cubic—Peng-Robinson equation of state in its modification by Melhem *et al*. [21]) to describe the phase equilibria of the

TABLE IV Comparison between experimental and calculated results for the partition coefficient $K^{(x)}$ of cardiac glycosides to coexisting high-pressure liquid phases in the ternary system CO_2 + water + 1-propanol.

p / MPa	$K^{(x)}$, experimental	$K^{(x)}$, calculated, full parameter set	$K^{(x)}$, calculated, reduced parameter set
digoxin, $T = 313.15$ K			
7.055	5.54	6.16	6.30
7.597	14.12	15.49	15.84
8.082	17.49	18.28	18.60
9.158	18.61	16.06	16.13
10.12	17.32	16.47	16.59
11.10	15.62	16.12	16.30
12.10	14.01	15.41	15.67
13.10	12.26	13.43	13.67
14.10	9.93	10.66	10.87
digoxin, $T = 333.15$ K			
10.11	5.02	5.29	4.99
11.08	10.72	10.88	9.84
11.59	13.07	12.96	11.58
12.10	13.96	13.14	11.56
13.10	13.70	13.76	12.04
14.11	12.20	12.87	11.17
15.10	10.59	11.25	9.73
16.12	7.83	8.65	7.47
digitoxin, $T = 313.15$ K			
7.059	7.43	8.98	10.49
7.597	19.47	16.59	18.14
8.058	27.74	29.01	31.43
9.098	36.38	34.10	35.54
10.10	40.52	35.92	37.19
11.10	42.44	37.70	38.23
12.10	43.24	38.64	38.65
13.10	40.33	38.37	38.33
14.10	35.40	36.45	36.56
digitoxin, $T = 333.15$ K			
10.10	6.87	7.18	6.95
11.10	20.98	16.71	16.45
12.10	32.14	24.99	25.56
13.10	36.11	29.09	29.76
14.10	36.36	32.24	33.06
15.10	32.65	32.48	32.48
16.10	25.74	30.98	32.41

ternary phase-forming system with an excess Gibbs energy (UNIQUAC-G^E) approach [22, 23] which is typically taken to correlate liquid-liquid equilibrium data at normal pressures. The finding that a "liquid-liquid tie-line" of a L_1L_2V-equilibrium at different pressures but at the same temperature resembles a standard isothermal low-pressure liquid-liquid equilibrium on projection into a single triangular diagram brought Adrian to apply this combination despite of that crude approximation. So, the correlation procedure was done in three steps: firstly, to correlate the L_1L_2 V-equilibrium of the ternary system with the equation of state to obtain the pressure for the isothermal L_1L_2 V-equilibrium, secondly, to correlate the liquid-liquid tie-lines of the ternary system with the UNIQUAC-G^E-model (for the associated six UNIQUAC interaction parameters of our phase-forming components see [19]), thirdly and finally comes the correlation of the partition coefficient of the fourth component on coexisting liquid phases, only taking into account the isoactivity criterion for the fourth component. The UNIQUAC size (r) and surface parameters (q) were as follows: $r = 13.9224$ and $q = 10.662$ for digoxin and $r = 13.7729$ and $q = 10.526$ for digitoxin [9]. The experimental partitioning data are used to calculate binary UNIQUAC interaction parameters a_{12}, which are given in Table V, between the solute (1) and the members of the phase-forming system (2) by a fitting routine. Alternatively, Adrian proposed to reduce the number of parameters by setting the interaction parameter of the biocompound with the phase-forming components $a_{12} = 10000$ (i.e., ∞ in Table V). In the case of digoxin a_{12} for 2 = water was kept and a_{21} for 2 = CO_2 set 10000 instead, but therefore, caution shall be exercised with this simplification in any case. The results shown in Figs. 7 and 8 prove that the mean relative deviation does not exceed $\approx$ 12% as found for digitoxin.

Another correlation solely based on the Peng-Robinson equation of state [24] and hence avoiding the combination of two models has been recently developed by Freitag *et al*. and applied to that system [25]. Further improvement of the correlation method especially withdrawing several approximations is the focus of further research.

TABLE V UNIQUAC interaction parameters a_{mn} between the biomolecule (1) and a phase-forming component (2).

	Phase-forming component (2)					
	CO_2		water		1-propanol	
Biomolecule (1)	a_{12}/K	a_{21}/K	a_{12}/K	a_{21}/K	a_{12}/K	a_{21}/K
Full parameter set						
Digoxin	898.3	947.8	83.54	−273.6	616.4	−457.7
Digitoxin	80.82	304.5	90.40	−617.5	288.8	−640.2
Reduced parameter set						
Digoxin	∞	∞	40.00	−398.8	∞	−657.2
Digitoxin	∞	−210.7	∞	−723.8	∞	−736.4

4. Conclusions

If supercritical fluids are to be consulted for process development in an extraction process or in a gas antisolvent process [26], to cite two applications only, the big challenge which has to be mastered before any process goes into operation is high-pressure phase behavior. Our work is dedicated to the principle that experimental and theoretical work is equally important for the right understanding. A further statement which we attach much importance to is that modelling shall be more than a phenomenological description of experimental data with a number of parameters but be based on a consistent physical and thermodynamic fundament.

We tried to correlate our results with a different model for each of the two phase systems investigated. The correlation of the high-pressure solubility data of the anthraquinone derivatives proved capability to describe both the low- and high-pressure regime. Retrograde solubility could be described, and the parameters have a consistent physical meaning. Therefore, we think it is possible to derive thermophysical properties (e.g., saturation pressure) as a first approximation [11, 15, 16]. The hybrid model employed for correlating the infinite dilution partition of the digitalis glycosides is an example for the difficulties you face when dealing with multicomponent systems. The model, however, is able to describe the partitioning behavior quite well, but it is not completely consistent and requires further effort for improvement. The aim is to develop new models which can both describe "real systems" and keep physically correct at the fundamental level.

Acknowledgements

The authors thank the Deutsche Forschungsgemeinschaft (DFG) and the Fonds der Chemischen Industrie e. V. for financially supporting this work. T. K. also acknowledges the support by the Arbeitsgemeinschaft industrieller Forschungseinrichtungen (AiF) and the Bundesministerium fur Wirtschaft und Technologie.

References

1. G. BRUNNER (ED.), Supercritical Fluids as Solvents and Reaction Media (Elsevier, Amsterdam, San Diego, Oxford, London, 2004).
2. K. LEONHARD and T. KRASKA, *J. Supercrit. Fluids* **16** (1999) 1.
3. T. KRASKA, K. O. LEONHARD, D. TUMA and G. M. SCHNEIDER, *J. Supercrit. Fluids* **23** (2002) 209.
4. T. ADRIAN, M. WENDLAND, H. HASSE and G. MAURER, *J. Supercrit. Fluids* **12** (1998) 185.
5. K. RIAZ and A. D. FORKER, *Drugs* **55** (1998) 747.
6. G. G. BELZ, K. BREITHAUPT-GROGLER and U. OSOWSKI, *Eur. J. Clin. Invest.* **31**, Suppl. 2 (2001) 10.
7. P. SWIDERSKY, D. TUMA and G. M. SCHNEIDER, *J. Supercrit. Fluids* **9** (1996) 12.
8. P. SWIDERSKY, Spektroskopische Hochdruckuntersuchungen zur Löslichkeit von Anthrachinonfarbstoffen in überkritischen Gasen bei Drücken bis zu 180 MPa und Temperaturen zwischen 300 K und 360 K (Dissertation, Ruhr-Universität Bochum, 1994; Shaker, Aachen, 1994).
9. T. ADRIAN, Hochdruck-Mehrphasengleichgewichte in Gemischen aus Kohlendioxid, Wasser, einem wasserlöslichen organischen Lösungsmittel und einem Naturstoff (Dissertation, Universität Kaiserslautern, 1997).
10. T. ADRIAN, J. FREITAG and G. MAURER, *Biotechnol. Bioeng.* **69** (2000) 559.
11. T. KRASKA, J. JURTZIK, D. TUMA and G. M. SCHNEIDER, *Russ. J. Phys. Chem.* **77** (2003) S51.
12. D. TUMA, B. WAGNER and G. M. SCHNEIDER, *Fluid Phase Equilibria* **182** (2001) 133.
13. R. SPAN and W. WAGNER, *J. Phys. Chem. Ref. Data* **25** (1996) 1509.
14. D. TUMA and G. M. SCHNEIDER, *Fluid Phase Equilibria* **158-160** (1999) 743.
15. S. GARNIER, E. NEAU, P. ALESSI, A. CORTESI and I. KIKIC, *Fluid Phase Equilibria* **158–160** (1999) 491.
16. T. KRASKA, K. O. LEONHARD, D. TUMA and G. M. SCHNEIDER, *Fluid Phase Equilibria* **194–197** (2002) 469.
17. G. M. SCHNEIDER, D. TUMA, M. WINTER and B. WAGNER, *Z. Kristallogr., NCS* **216** (2001) 299.
18. T. ADRIAN, S. OPRESCU and G. MAURER, *Fluid Phase Equilibria* **132** (1997) 187.
19. T. ADRIAN, J. FREITAG and G. MAURER, *J. Supercrit. Fluids* **17** (2000) 197.
20. T. ADRIAN, J. FREITAG and G. MAURER, *Ind. Eng. Chem. Res.* **40** (2001) 4990.
21. G. A. MELHEM, R. SAINI and B. M. GOODWIN, *Fluid Phase Equilibria* **47** (1989) 189.
22. D. S. ABRAMS and J. M. PRAUSNITZ, *AIChE J.* **21** (1975) 116.
23. G. MAURER and J. M. PRAUSNITZ, *Fluid Phase Equilibria* **2** (1978) 91.
24. J. FREITAG, Hochdruck-Mehrphasengleichgewichte in Systemen aus Wasser, einem organischen Lösungsmittel und (nahekritischem) Ethen (Dissertation, Universität Kaiserslautern, 2003; Cuvillier, Göttingen, 2003).
25. J. FREITAG, D. TUMA and G. MAURER, *Chem.-Ing.-Tech.* **75** (2003) 142.
26. A. WEBER, L. V. YELASH and T. KRASKA, *J. Supercrit. Fluids*, **32** (2005) 107.

Received 16 August 2004
and accepted 13 April 2005